# In-beam electron conversion from high-spin states in $^{203}$Pb

Richard J. McDonald and James E. Draper
*Crocker Nuclear Laboratory and Physics Department, University of California, Davis, California 95616*
(Received 8 June 1978; revised manuscript received 30 May 1979)

In-beam, time-sorted measurements of internal conversion electrons and $\gamma$ rays are reported for $^{203}$Pb formed by the $^{204}$Hg $(\alpha,5n)$ reaction at $E_\alpha = 53.5$ MeV. The multipolarity of the 153 keV transition deexciting the $29/2^-$ isomer is determined to be $E3$. The 239-keV transition, in the cascade connecting the $23/2^+$ and $21/2^+$ states, is determined to be $M1$. The 874-keV transition is found to have an $M1/E2$ $\gamma$ intensity ratio of $0.4^{+0.20}_{-0.15}$. Thus, the state at 2796 keV is assigned $J^\pi = 23/2^+$ and has a probable configuration $p_{1/2}{}^{-1}f_{5/2}{}^{-3}i_{13/2}{}^{-1} + p_{1/2}{}^{-2}f_{5/2}{}^{-1}f_{7/2}{}^{-1}i_{13/2}{}^{-1}$. The other measured multipolarities are $E2$(258 keV), $M1$(635 keV), $E2$(839 keV), and $M4$(1027 keV) with no measurable admixture of multipoles.

[NUCLEAR REACTIONS $^{204}$Hg$(\alpha,5n)^{203}$Pb, $E_\alpha = 53.5$ MeV. Measured $\gamma$ and conversion electron spectra 30–1300 keV in eight time bands between beam bursts. Deduced ICC, $J$, $\pi$. Si(Li) and Ge(Li) detectors.]

Recent studies of Pb nuclei near $^{208}$Pb, have shown that rather simple wave functions account for many of the experimental results. This is particularly true of the three-hole $^{205}$Pb, studied by the Stockholm group.[1] The more recent reports[2-4] on $^{203}$Pb have illustrated the considerably greater difficulty involved in comprehensive understanding of this five-hole nucleus.

The decay sequences in $^{203}$Pb, produced in-beam by $(\alpha, xn)$ reactions, have been fairly well settled by the work of Lindén[3] and the work of Saha *et al.*[4] However, the crucial assignment of spins and parities $(J^\pi)$ of transitions and levels still contains several ambiguities, since there have been no clean, direct measurement of $J^\pi$ for transitions in $^{203}$Pb below ~600 keV. The $J\pi$'s of some lower transitions have been inferred[3,4] from combinations of indirect measurement ($\gamma$ intensity balance) and physical arguments for deciding between alternatives consistent with those indirect measurements. However, the direct measurement of internal conversion coefficients (ICC's) of these transitions, for the various shells, is needed to provide a firm experimental determination of $J\pi$ to compare with theoretical models. Such measurements are reported here.

Figure 1 shows the most intense transitions in $^{203}$Pb stemming from in-beam $(\alpha, xn)$ reactions. The work of Saha *et al.*[4] is with $^{202}$Hg $(\alpha, 3n)$ $^{203}$Pb at 38 MeV. The work of Lindén[3] is with $^{204}$Hg $(\alpha, 5n)$ $^{203}$Pb at 45–55 MeV. Lindén measured excitation functions, and both works utilized $\gamma$-$\gamma$ coincidences and time distributions to place the transitions into decay sequences, shown in Fig 1. Apart from the order of the 635- and 239-keV transitions, those decay sequences are in agreement.

For the crucial question of the $J^\pi$ of the levels, Lindén directly measured ICC's, the lowest $^{203}$Pb transition for which $\alpha_K$ was measured being 634 keV, and the lowest transition energy with relatively clean electron data being at 374 keV in $^{204}$Pb. Saha *et al.* utilized angular distributions (which give no information about parity) for the 839- and 258-keV transitions only. Both works used intensity balances of $\gamma$ rays to infer the sum of $K$, $L$, $M, \ldots$, ICC's for the 239- and 153-keV transitions, and from these inferred the $J\pi$'s. Such an inference of ICC's presumes that there are no competing, strongly converted transitions whose $\gamma$'s were unrecognized.

Furthermore, since only the sum of $K$, $L$, $M, \ldots$, ICC's was deduced by them, uncertainties about $J\pi$ can result, as was the case for the 153-keV transition from the highest-spin state observed. The theoretical total-conversion coefficients[5,6] for 153 keV are 16.0 for $E3$ and 16.9 for $M2$, differing by only 5%. From this, for the 153-keV transition, Saha *et al.* favor $E3$, while Lindén lists $M2$ in his abstract. Thus, they favored different spins for the 2796-keV level.

Another example of the ambiguities from total ICC alone, is in the 239-keV transition of Fig. 1. Saha *et al.* infer $\alpha_{tot} = 0.66 \pm 0.18$, while Lindén finds $1.1 \pm 0.6$. These do not clearly distinguish between $E3$ and $M1$, whereas our measurements of $\alpha_K$ and the $K/L$ ratio do so easily.

Since there is so little direct information about ICC's $\lesssim$ 500 keV for in-beam transitions in $^{203}$Pb, the present work reports direct measurements of those conversion electrons and ICC's for the electron energy range ~60–1200 keV. In addition to the question of low-energy transitions, the $\alpha_K$

 

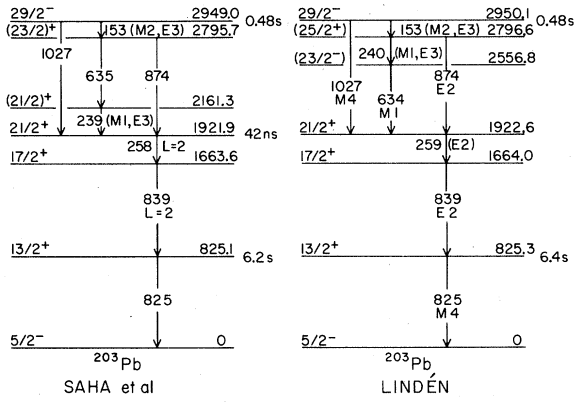


FIG. 1. Level schemes, related to the present work, proposed by Saha *et al.* (Ref. 4) (left) and Linden (Ref. 3) (right). Transition multipolarities are included only where the experimental results were unambiguous, without recourse to models.

(874 keV) is reported here to be double that measured by Lindén, indicating significant mixing of $E2$ and $M1$.

## EXPERIMENTAL METHODS

$^{203}$Pb was formed using the $(\alpha, 5n)$ reaction on $^{204}$Hg-enriched HgO targets and 53.5-MeV $\alpha$ particles generated by the 193-cm isochronous cyclotron at this laboratory. The targets contained 93% $A = 204$, 5% $A = 202$, 1% $A = 201$, and 1% $A = 200$. In our various experiments, time-sorted $\gamma$ rays over the region 100–1300 keV, conversion electrons over a similar region, and conversion electrons over the region 30–500 keV were measured. Target thicknesses of ~5, 0.8, and 0.6 mg/cm$^2$, respectively, were used. In addition, $\gamma$ spectra were taken with only the aluminized Mylar backing of the target in order to obtain background. Eight time bands covered 83 of the 96 ns separating beam bursts from the cyclotron. The $\gamma$-ray data were taken with a 22-cm$^3$ Ge(Li) crystal.

The electron data were taken with a 3-mm thick Kevex Si(Li) detector. This Si(Li) detector is a part of our in-beam electron spectrometer.[7] Briefly, this spectrometer consists of a solenoidal magnet, a helical Pb baffle for positron and photon rejection, and the cooled Si(Li) detector. System resolution is ~2.5 keV at 624 keV ($^{137}$Cs). The spectrometer has a moderate bandpass (~19% in momentum), and a computer-control system sweeps the solenoid current linearly to cover the desired energy interval. Corrections must be applied to the raw electron data[7-10] to account for several effects, the most important of which are (1) low-energy electrons scattering, in the target, out of the solenoid acceptance angle, and (2) dead time which varies with count rate. All

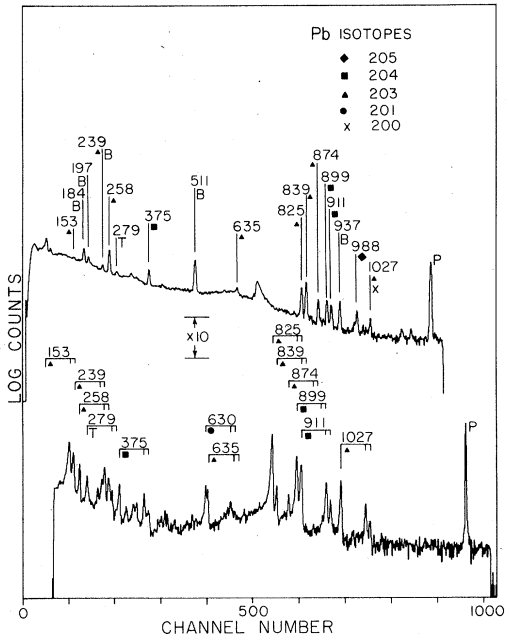


FIG. 2. Delayed $\gamma$ (top) and conversion electron (bottom) spectra showing isotopic identities. Also, $B$ = background, $T$ = Pb → Tl radioactive decay, $P$ = electronic pulser. The size of a decade is shown in the insert.

corrections discussed in Refs. 7–10 are included in this work, but are not discussed individually here.

## RESULTS

Figure 2 shows low-gain spectra of $\gamma$'s and electrons. Figure 3 shows the conversion electrons of low energy. The experiments cover a range of electron energies from 60 to 1200 keV. Table I and Figs. 4 and 5 show the intensities of the various transitions and the ICC's. The ICC's are normalized to the theoretical[5] ICC of the $M4$ 825-

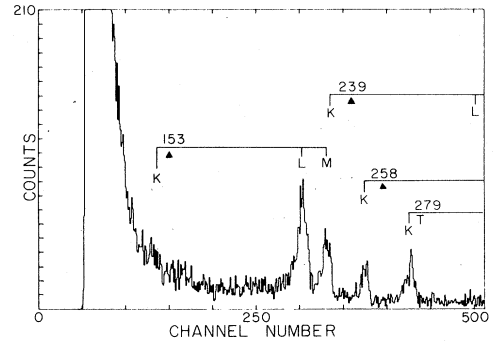


FIG. 3. Low-energy, conversion-electron spectrum. Symbols for line identification are the same as in Fig. 2.

TABLE I. Relative intensities and ICC's in $^{203}$Pb from this work.

| Transition energies (keV) | $I_\gamma$ (total) [a] | $I_\gamma$ (del'd) [b] | $I_K$ (del'd) [b] | $\alpha_K$ [c] | $K/L$ [d] | $I_\gamma(1+\alpha_T)$ [e] | $J\pi$ [d] |
|---|---|---|---|---|---|---|---|
| 153.2 | 3.9±0.5 | 3.9±0.5 | 38.6 ±3.0 [f] | $\alpha_L$=9.9 ±1.5 | <0.7 | 51.4±6.4 | $E3$ |
| 239.1 | 10.5±2.1 | 9.0±1.9 | 7.9 ±2.0 | 0.88 ±0.29 | 7 ±1 | 15.0±3.0 | $M1$ |
| 258.4 | 82 ±5.8 | 83 ±5.7 | 6.2 ±0.70 | 0.074 ±0.010 | 1.2±0.10 | 75.8±5.5 | $E2$ |
| 634.8 | 15.4±1.7 | 13 ±1.9 | 0.69±0.10 | 0.053 ±0.011 | 5.8±1.3 | 12.7±1.5 | $M1$ |
| 825.0 | 100 ±8.2 | 100 ±6.7 | 22.0 ±1.2 | 0.22 ±0.019 | ··· | 100 ±8.3 | $M4$ |
| 838.6 | 117 ±8.2 | 95 ±6.7 | 0.78±0.12 | 0.0082±0.0014 | ··· | 92 ±6.4 | $E2$ |
| 873.8 | 31.0±2.3 | 26.7±1.6 | 0.29±0.030 | 0.011 ±0.0013 | 6.1±1.4 | 24.4±1.8 | $E2+M1$ [g] |
| 1026.8 | 8.0±1.2 | 8.0±0.95 | 0.85±0.10 | 0.106 ±0.018 | 3.9±0.40 | 7.1±1.0 | $M4$ |

[a] Total intensity, summed over all time bands.
[b] del'd means everything with half-life >20 ns.
[c] ICC normalized to $M4$ for 825 keV.
[d] See Figs. 4 and 5 for comparison with theory.
[e] Transition intensities summed over all time bands and renormalized. The $\alpha_T$ uses our experimental values when available, otherwise Refs. 5 and 6.
[f] $L$ conversion intensity.
[g] $\gamma$ intensity ratio $M1/E2$ is $\delta^2 = 0.4^{+0.20}_{-0.15}$.

keV transition.[2]

For the 153-keV transition, $\alpha_L$ was measured to be 9.9 ± 1.4. As shown in Fig. 3, the $K$ line is very weak compared to the $L$ and $M$ lines. After correction for overall spectrometer efficiency, the upper limit of the $K/L$ ratio is <0.7. These data strongly support an $E3$ assignment for the 153-keV transition, since the $K/L$ ratio for $M2$ is 3, Fig. 5.

From the experimental $\alpha_K$ and $K/L$ ratio for the 239-keV transition, it is determined to be $M1$. There is extra difficulty in this measurement since: (1) The 239-keV $K$ line lies at about the same energy as the 153-keV $M$ line, and (2) The $\gamma$ is partially obscured by the ~239-keV transition in $^{19}$Ne. The $L/M$ ratios are relatively insensitive

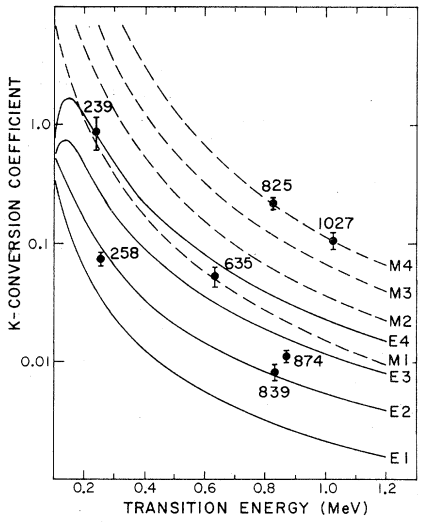


FIG. 4. Experimental $K$-conversion coefficients compared to theory (Ref. 5).

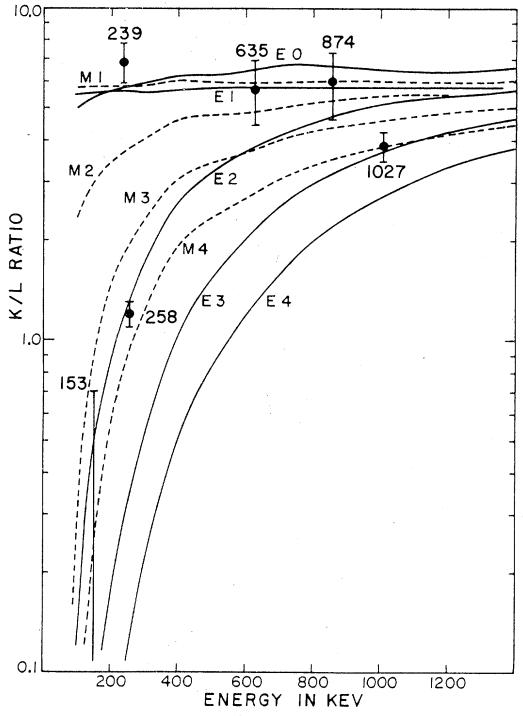


FIG. 5. Experimental $K/L$ conversion ratios compared to theory (Ref. 5). The entry for the 153-keV transition is an upper limit since no evidence for the $K$ peak appears in Fig. 3.

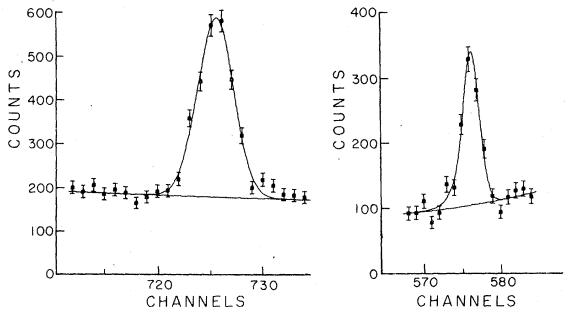


FIG. 6. The computer-aided, least-squares fits for the 873.8-keV $\gamma$ (on the left) and its $K$ conversion electron (on the right). The latter has a width of 3.4 keV at half-maximum.

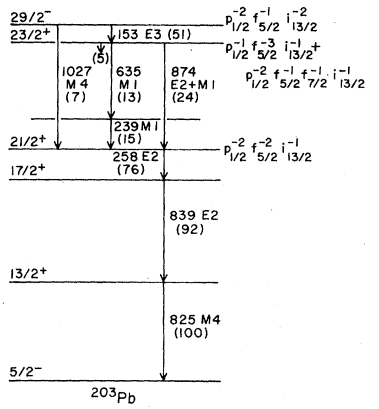


FIG. 7. Results of this work. The transition intensities, in parentheses, are summed over all time bands. The sequence of the 635- and 239-keV transitions is not determined, experimentally. The intensity of 5 for other transitions from the $\frac{29}{2}^+$ state is deduced from Ref. 4.

to multipolarity, so an $L/M$ ratio of 3.6 for 153 keV was used to obtain the 153-keV $M$ intensity for subtraction from the total peak area to obtain the 239-keV $K$ line. The "background" run on the Al-Mylar target backing was used to determine that part of the $\gamma$ intensity due to $^{203}$Pb. The individual time bands were used in making this subtraction.

The 1027-keV transition was measured to be $M4$, Figs. 4 and 5. This $\gamma$ has a contaminant ($\sim 10\%$) from $^{200}$Pb. Previously measured[9] intensity ratios were used in correcting for this contaminant.

Figures 4 and 5 indicate that the 874-keV transition is intermediate between $E2$ and $M1$. The $\alpha_K$ in Table I is double that of Lindén. However, examination of the electron spectrum in Fig. 8 of Ref. 3 suggests considerable uncertainty in that electron intensity. Furthermore, the 874-keV $L$ peak in Fig. 2 is too weak for a doubled $\alpha_K$. Figure 6 shows the least-squares computer fits for the present data, resulting in an $M1/E2$ mixing ratio (of $\gamma$ intensities) of $\delta^2 = 0.40\ ^{+0.20}_{-0.15}$. The expected $K/L$ ratio is 5.4 which is consistent with the experimental result as in Fig. 5. The only way that this large $M1$ admixture could be an artifact, would be the undetected presence in Fig. 6 of another transition with an energy within $\lesssim 1$ keV and strongly converted. The width of the electron peak in Fig. 6 is the same as the computer-fitted peaks nearby to within $\pm 0.4$ keV.

Figures 4 and 5 show that the 239-keV transition is $M1$ rather than $E3$. In Refs. 3 and 4 there was no certain experimental basis for distinguishing between $M1$ and $E3$.

Similarly, Figs. 4 and 5 show that the 258-keV transition is $E2$. This confirms the assignment made in Ref. 3 from the $\gamma$ intensity balance and $\alpha_L$; in Ref. 4 $L = 2$ was found.

The present results cannot distinguish between the coincidence sequences 239 keV to 635 keV proposed by Lindén[3] and 635 keV to 239 keV proposed by Saha *et al.*[4] Table I shows essentially the same prompt and delayed intensities for each of those two transitions. The same conclusion holds for the measured $I_\gamma$ for those two transitions in Refs. 3 and 4, when $\alpha \simeq 1$ is considered for the 239-keV transition. Several weak $\gamma$ transitions observed by Saha *et al.*[4] were used to support their conclusion that the 239-keV transition is lower in the cascade.

Figure 7 summarizes our results on the $J^\pi$ of levels in the decay sequence of Fig. 1.

## DISCUSSION

Since $^{203}$Pb is 5 neutron holes away from $^{208}$Pb, no extensive shell model calculation has yet been made. The residual interactions between so many holes make the full calculation too complex. There have been attempts to describe odd-$A$ nuclei in this region with a weak-coupling model[11] in which a hole is coupled to a vibrating core. In another model,[12] some states are described as single-particle Nilsson states with an oblate core. In Ref. 13 the core is a tri-axial rotor. However, these theories do not account for many properties of levels in nuclei as far from $^{208}$Pb as the present $^{203}$Pb.

Lindén[3] used the zero-order energies (noninteracting holes) and the experimental $^{205}$Pb levels to suggest a $\frac{29}{2}^- \xrightarrow{M4} \frac{21}{2}^+$ isomeric transition of $\sim 1$ MeV, which motivated his work. This is probably the 1027-keV transition shown in Figs. 1 and 7. Figure 7 shows Lindén's suggestion for the dominant configuration in the wave functions of those two states, $\frac{29}{2}^-$ and $\frac{21}{2}^+$. The $M4$ transition is then $i_{13/2}{}^{-1} \rightarrow f_{5/2}{}^{-1}$, which is the only $M4$ possibility

among the single-particle hole states in $^{207}$Pb.

What is the configuration of the $\frac{23}{2}^+$ state? If the transitions are predominately single-particle, rather than collective, then in order to have $\frac{29}{2}^- \xrightarrow{E3} \frac{23}{2}^+$, the only reasonable component of the $\frac{23}{2}^+$ state is $p_{1/2}^{-2} f_{5/2}^{-1} f_{7/2}^{-1} i_{13/2}^{-1}$. Although in zeroth order that component is ~0.7 MeV above the $\frac{29}{2}^-$ state, only a weak admixture is needed to account for the otherwise-forbidden single-particle $E3$ decay. That same component of the wave function can also produce the $M1$ component of the transition to the $\frac{21}{2}^+$ state, as in Fig. 7, if the $E2$ component is not too strongly enhanced. In zeroth order, the lowest-energy component of the $\frac{23}{2}^+$ state is $p_{1/2}^{-1} f_{5/2}^{-3} i_{13/2}^{-1}$ which can account for the $\frac{23}{2}^+ \xrightarrow{E2} \frac{21}{2}^+$ transition. However, that component alone in the $\frac{23}{2}^+$ state would not permit the $\frac{29}{2}^- \xrightarrow{E3} \frac{23}{2}^+$ transition.

Richel *et al.*[2] and Saha *et al.*[14,4] discuss the interpretation of levels in $^{203}$Pb in terms of an $i_{13/2}$ neutron hole coupled to the experimental states of $^{204}$Pb. There is some experimental evidence favoring this model, but experimental results on other matrix elements are also needed to further define the wave functions.

This work was supported, in part, by the National Science Foundation.

[1]C. G. Lindén, I. Bergström, J. Blomqvist, K. G. Rensfelt, H. Sergolle, and K. Westerberg, Z. Phys. A277, 273 (1976).
[2]H. Richel, G. Albouy, G. Auger, J. C. David, J. M. Lagrange, M. Pautrat, C. Roulet, H. Sergolle, and J. Vanhorenbeeck, Nucl. Phys. A267, 253 (1976).
[3]C. G. Lindén, Z. Phys. A280, 51 (1977).
[4]S. K. Saha, H. Helppi, P. J. Daly, S. R. Faber, T. L. Khoo, and F. M. Bernthal, Phys. Rev. C 16, 2159 (1977).
[5]R. S. Hager and E. C. Seltzer, Nucl. Data 4, 1 (1968).
[6]O. Dragoun, Z. Plajner, and F. Schmutzler, Nucl. Data A9, 119 (1971).
[7]J. E. Draper, R. J. McDonald, and W. G. Wyckoff, Nucl. Instrum. Methods 151, 135 (1978).
[8]J. E. Draper, R. J. McDonald, and N. S. P. King, Phys. Rev. C 16, 1594 (1977).
[9]R. J. McDonald and J. E. Draper, Phys. Rev. C 17, 944 (1978).
[10]R. J. McDonald, Ph.D. thesis, University of California, Davis, 1977, University Microfilms Order No. 78-9241 (unpublished).
[11]L. Silverberg, Ark. Fys. 20, 355 (1961).
[12]J. O. Newton, N. Cirilov, F. S. Stephens, and R. M. Diamond, Nucl. Phys. A148, 593 (1970).
[13]J. Meyer-ter-Vehn, Nucl. Phys. A249, 111 (1975); A249, 141 (1975).
[14]H. Helppi, S. K. Saha, P. J. Daly, S. R. Faber, T. L. Khoo, and F. M. Bernthal, Phys. Lett. 67B, 279 (1977).